

USING DETERMINISTIC METHODS FOR RESEARCH REACTOR STUDIES

E. VARIN, S. NOCEIR, R. ROY, D. ROZON

Institut de Génie Nucléaire, École Polytechnique de Montréal
P. O. Box 6079, Station Centre ville, Montréal, Québec H3C 3A7 CANADA
E-mail: varin@meca.polymtl.ca

and

C. GUERTIN

Énergie Atomique du Canada Limitée
1155 Metcalfe, Montréal, Québec H3B 2V6 CANADA

Abstract — As an alternative to prohibitive Monte Carlo simulations, deterministic methods can be used to simulate research reactors. Using various microscopic cross section libraries currently available in Canada, flux distributions were obtained from DRAGON cell and supercell transport calculations. Then, homogenization/condensation is done to produce few-group nuclear properties, and diffusion calculations were performed using DONJON core models. In this paper, the multigroup modular environment of the code DONJON is presented, and the various steps required in the modelling of SLOWPOKE hexagonal cores are described. Numerical simulations are also compared with experimental data available for the EPM Slowpoke reactor.

I. INTRODUCTION

Most research reactors have small and highly heterogeneous cores. Thus, leakage effects out of these cores are generally difficult to predict. To study the core behavior, one usually performs numerous simulations using probabilistic methods. However deterministic methods with similar simulation capabilities allow these studies to be less time consuming. In these approaches, a diffusion model of the core, along with its reflector and some structural material, is needed. Furthermore the nuclear properties must be obtained from a transport calculation, using a homogenization/condensation process for macroscopic cross sections and diffusion coefficients. Application of the usual multigroup transport/diffusion coupled simulations for research reactors is complicated by the fact that one must predict an accurate migration of neutrons throughout the core. Many diffusion codes are limited to a small number of energy groups which precludes their use for such research reactor studies.

Based on the TRIVAC-3 multigroup diffusion solver,^[1] the DONJON code has been extended to perform complex simulations in a user-friendly environment.^[2, 3] The code also allows solution on 3D Cartesian and hexagonal geometries, enabling users to perform simulations for various reactor types. Produced by the DRAGON transport code,^[4] multigroup nuclear properties can be used directly in DONJON. With these capabilities, DONJON is used in our effort to understand the High Enrichment Uranium (HEU)

Slowpoke-2 reactor at École Polytechnique.

The paper will summarize the evolution of the TRIVAC solver, with particular emphasis on its current use in research reactor studies. The simulation capability of the DONJON code will also be described. Numerical results will be given and compared with experimental data for HEU Slowpoke reactor. It will be shown that DRAGON/DONJON results are in reasonably good agreement with these experimental results.

II. DONJON CAPABILITIES

II.A. Hexagonal ADI solver

The TRIVAC code was developed to solve diffusion equation on Cartesian and cylindrical geometries with finite element or finite difference discretization. The one-speed diffusion equation can be discretized into an extended eigenvalue value problem of the form:

$$A\vec{\Phi} = \lambda B\vec{\Phi} \quad (1)$$

To solve this equation, matrix A must be inverted. As this matrix is sparse, the inversion process will fill it in and will be very time consuming. To avoid this problem, the TRIVAC solver uses the Alternating Direction Implicit (ADI) method. The ADI method is based on the interchangeability of the roles of mesh lines along each direction, leading to the splitting of the matrix A . The original version of TRIVAC solver uses ADI method on Cartesian geometries. Work was done to allow its use for 2D and 3D hexagonal geometries.^[5]

For these geometries, there are 4 non-orthogonal directions, X, Y, Z and W as shown in Figure 1. The fourth direction is used to access neighbours at 60°. In that case, the matrix A can be written as:

$$A = P_w U P_w^T + P_w W P_w^T + P_x X P_x^T + P_y Y P_y^T + P_z Z P_z^T \quad (2)$$

where

- U matrix containing the diagonal elements of A
- W, X, Y, Z matrices containing the coupling components of A along each axis
- P_w, P_x, P_y, P_z permutation matrices that will ensured that W, X, Y and Z have a diagonal banded structure.

Using ADI splitting, matrix A does not need to be explicitly constructed. Matrix assembly module creates four symmetric and diagonal banded matrices \tilde{X} , \tilde{Y} , \tilde{Z} and \tilde{W} such as :

$$\begin{aligned} \tilde{W} &= \tilde{W} + P_w^T U P_w \\ \tilde{X} &= \tilde{X} + P_x^T U P_x \\ \tilde{Y} &= \tilde{Y} + P_y^T U P_y \\ \tilde{Z} &= \tilde{Z} + P_z^T U P_z \end{aligned}$$

These four matrices composed an approximation of matrix A and are used to define the preconditioning matrix M as:

$$M = [P_z \tilde{Z}^{-1} P_z^T U] [P_y \tilde{Y}^{-1} P_y^T U] [P_x \tilde{X}^{-1} P_x^T U] [P_w \tilde{W}^{-1} P_w^T] \quad (3)$$

Matrices \tilde{X} , \tilde{Y} , \tilde{Z} and \tilde{W} are not explicitly inverted, but factorized with Choleski method.

The diffusion equation is solved using the preconditioned power method. This iterative method is described by the following algorithm:

$$\vec{\Phi}^{(1)} \quad \text{given} \quad (4)$$

$$\vec{\Phi}^{(k+1)} = \vec{\Phi}^{(k)} - M\{A\vec{\Phi}^{(k)} + \lambda^{(k)}B\vec{\Phi}^{(k)}\}; k > 1 \quad (5)$$

To obtain $\vec{\Phi}^{(k+1)}$, at least one ADI calculation per outer iteration is performed. It is normally enough to converge, but when systems are highly coupled the number of ADI calculations can be increased either at user demand or automatically by the code itself.

This method is accelerated with a two-parameter variational scheme. If we consider only one-speed equations, accelerated fluxes are given by:

$$\vec{\Phi}^{(k+1)} = \vec{\Phi}^{(k)} + \alpha^{(k)}\{\vec{g}^{(k)} + \beta^{(k)}(\vec{\Phi}^{(k)} - \vec{\Phi}^{(k-1)})\} \quad (6)$$

$$\vec{g}^{(k)} = -M\{\vec{\Phi}^{(k)} + \lambda^{(k)}A^{-1}B\vec{\Phi}^{(k)}\} \quad (7)$$

where $\alpha^{(k)}$ and $\beta^{(k)}$ are dynamically-calculated relaxation parameters.^[6]

The iterative strategy is composed of free and accelerated iterations. Free iterations are obtained with $\alpha^{(k)} = 1$ and $\beta^{(k)} = 0$. For accelerated iterations, $\alpha^{(k)}$ and $\beta^{(k)}$ are computed to minimize an appropriate functional. There are by default 3 free iterations followed by 3 accelerated ones.

II.B. Multigroup static calculations

The above resolution methods are used to solve multigroup diffusion equations as well. Partition between energy groups is made according to:

$$A_{gg}\vec{\Phi}_g = \sum_{\substack{h=1 \\ h \neq g}}^G A_{gh}\vec{\Phi}_h + \lambda \sum_{h=1}^G B_{gh}\vec{\Phi}_h \quad (8)$$

These equations are solved from the fastest to the slowest group because up-scattering matrices A_{gh} , for $h > g$, are generally zero matrices. This partition is represented as an example of 5 energy group problem in Figure 2. A_{gg} matrices are composed of the diffusion terms, which represent spatial coupling coefficients. These matrices are so splitted with ADI method as explained above. Scattering matrices A_{gh} only contain terms to transfer neutrons from one group to another and therefore have a diagonal form with respect to spatial discretization. Only diagonal values are then stored.

Table 1 shows the CPU time needed to compute a single diffusion solution on a CANDU-6 like reactor and on the HEU Slowpoke reactor. The Slowpoke-2 reactor representation involves a great number of regions per energy group in comparison with a CANDU reactor. As we can see, CPU time increases with the number of groups but stays in acceptable limits.

II.C. Extended capabilities: devices, detectors ...

To realize more advanced calculations involving different reactor configuration, features were added, such as device representation, detector responses and kinetics capabilities. A useful part of these new features is the possibility to define devices as geometrical parts of the core over the actual resolution geometry.

Therefore, device geometric definitions and movements are independent of the resolution geometry, and they do not affect their incremental cross sections. Devices in Cartesian geometries are easy to define as a set of coordinates in the geometry axis. For hexagonal geometry, elements in each Z plane are numbered from the center to the outside region in circle. In this context, it is simple to access hexagons by their number instead of coordinates. Hexagonal devices are also defined by their actual coordinates along Z-axis and by the number of hexagons they occupy in the complete geometry. They are supposed to occupy totally at least a hexagon.

DONJON also allows movement and control of such devices during a simulation with respect to user-defined algorithms. Actual position of a device is set in terms of fraction of full positions. For example, if a Cartesian device moves along Y axis, its present position in fraction will be :

$$Pos(\%) = 100. \times \frac{Y_{max}^{cur} - Y_{ref}}{Y_{max} - Y_{ref}} \quad (9)$$

where Y_{max} is the maximal position of the device, Y_{ref} the origin of Y axis and Y_{max}^{cur} the actual maximal position along Y axis. Speeds in fraction of full speed can also be defined with respect to a maximal speed allowed for the device. Devices can only move along one existing axis of the geometry.

For any device type in the proper corresponding resolution geometry, the mesh properties are obtained by adding a compound fraction of device properties over the original cell properties:

$$\Sigma_g^{[mesh]} = \Sigma_g^{[cell]} + f \times (\Sigma_g^{[device\ in]} - \Sigma_g^{[device\ out]}) \quad (10)$$

where f is the volumetric fraction occupied by the device in the cell.

When a device is moved, the cells it affects are reestablished as well as the volumetric fraction of each of them. This allows simulations to be realized without paying any particular attention to the device positions along with time.

Detectors can also be used in simulations as flux indicators for regulation capability or as flux reference point. Like a device, a detector is defined by coordinates for Cartesian and cylindrical geometries or by hexagon numbering for hexagonal ones. With these geometrical informations, flux interpolation can be performed to recover it at a special site. Spectral informations must be given to the detectors according to their sensibility in order to recover a single value representing the actual detector response.

When using for regulation capability, detector responses are generally computed in fraction of full power with respect to a referenced state. But they can also be used to input a flux value at a special point and then using this value to normalize the overall fluxes in order to obtain reactor power. In this case, the normalization factor is :

$$f_n = \frac{\Phi_d^{fixed}}{\Phi_d^{comp}} \quad (11)$$

The corresponding reactor power will be computed as:

$$P = \langle H\Phi \rangle \times f_n \quad (12)$$

This capability is very useful to follow the power excursion in a transient and then compare it with measured data.

III. DRAGON USE FOR PROPERTY GENERATION

The lattice code DRAGON was used to obtain macroscopic energy dependent cross sections for DONJON calculations. Those properties must be computed to respect the diffusion theory, i.e. using a homogenization/condensation process for macroscopic cross sections and diffusion coefficients. To accurately take care of the leakage effects, DRAGON computations are realized using B_1 homogeneous model. In this model, total cross sections are corrected to include leakage effects such as:

$$\Sigma_{t,g}^{cor} = \Sigma_{t,g} + d_g B^2 \quad (13)$$

where B^2 is the buckling, and d_g are the group-dependent leakage coefficients.

With a first estimate of the correction to the total cross sections, the eigenvalue problem is solved. At each outer iteration, a new buckling value B^2 is computed using the homogenized cell or supercell properties, then leakage coefficients d_g are calculated. Absorption cross sections are corrected by the streaming term $d_g B^2$ and a new solution to the eigenvalue problem is computed. These iterations end when K_{eff} reaches 1.0. The final buckling is used to compute diffusion coefficients for core calculations. Nuclear properties can then be homogenized and condensed to a few energy groups.

For HEU Slowpoke reactor, the transport core model is a 2D cluster that represents each different material. Proper core conditions, such as material temperatures, are also set. So new calculations have to be done for each new core condition. Microscopic libraries such as Winfrith or ENDF-B libraries from AECL can be used. When the transport equation is solved and the material regions are homogenized, informations are stored to produce condensation of the macroscopic properties. Different final number of groups can be considered by condensing the initial energy band of 0. to 10 Mev. As illustrated in Table 2, the energy cut has been made to obtain an equal number of groups in the thermal and fast spectrum.

The resulting macroscopic properties are stored in the COMPO files. This type of file has been developed to unify output storage and to be able to keep macroscopic as well as microscopic cross sections with a variable number of energy groups and for different burnup steps. The COMPO files are directly accessed in the DONJON computation to insure adequate data flow.

IV. HEU SLOWPOKE-2 SIMULATIONS

IV.A. Previous work

Temperature reactivity measurements were carried out at École Polytechnique in 1987. Guertin^[7] attempted to reproduce these coefficients using WIMS-CRNL,^[8] DRAGON and

TRIVAC codes. As in many research reactors, the HEU Slowpoke-2 reactor has a hexagonal core with a reflector composed of a beryllium annulus pierced by five irradiation sites. This study was carried out using a previous version of TRIVAC which solved the diffusion equation for only two energy groups, without any up-scattering effect. Only Cartesian or cylindrical geometries were available. The HEU Slowpoke-2 was then represented as an R-Z geometry where fuel and irradiation sites were smeared into cylindrical zones. Macroscopic properties were generated from WIMS-CRNL based on the 69-group WIMS-AECL microscopic library, and detailed studies were done with DRAGON in order to determine the behavior of water holes in the core (using double heterogeneity).^[7]

These two energy group simulations gave reactivity far above the critical condition of the HEU core. These results were essentially due to the sub-moderation inside the reactor that could not be represented with the 2 energy group model. Nevertheless, negative temperature feedback behavior was successfully reproduced. The need for a full multigroup approach to the problem and for a more accurate representation of the core geometry was demonstrated.

IV.B. Reactor representation in DONJON

The capability of hexagonal geometry in DRAGON and DONJON codes allows a more accurate representation of the HEU Slowpoke reactor. In DONJON, the 3D hexagonal model of the reactor is composed of the core, its reflector and part of the light-water pool surrounding the core. Static calculations in the DONJON code are performed. To improve the reactor model, the number of energy groups and the spatial discretization were looked at, in order to find converged values where fluxes and multiplication factor are stable.

To separate the different materials along the Z axis, 9 planes are required. In this case, the light-water zones on top and bottom of the core are represented as two planes, so reflector conditions are not well taken into account. The number of Z planes was increased to 13, in splitting the water regions. It was necessary to increase the number of Z-planes to insure an accurate value of the initial core criticality. When the number of planes is increased, the multiplication factor decreased. From 20 Z planes, K_{eff} is almost stable. The converged reactor geometry is so composed of 31 concentric crowns of hexagons per Z plane, for 20 planes. The total number of unknowns per energy groups is ≈ 60000 . This study was done with only two energy groups because of memory limitations.

The number of energy groups, N_g , used in DONJON has also been changed to find an optimum between CPU time and required storage while representing an accurate behavior of the reactor. In this context, values of N_g from 2 to 8 were considered with the available AECL microscopic libraries (WIMSLIB, ENDF/B5, ENDF/B6). Calculations for 10 and 12 energy groups were also performed but were limited to 13 Z-planes. Fig. 3 shows that there is no need to go beyond 6 energy groups. Above that, the reactivity is almost constant, although CPU time increases significantly.

The HEU Slowpoke-2 reactor is controlled by a single aluminium sheathed rod. This rod is 38 cm high and is composed of two aluminium spacers and a cadmium absorber. Nuclear properties of the rod were also computed with DRAGON. The rod is represented as two regions, one for the absorber and one for its guide tube. In DONJON, the rod is

placed in the 7 central hexagons of the affected planes. As it was early mentioned, it can be moved to affect different planes of the reactor.

For 6 energy groups with no control rod, Fig. 4 shows the most thermal flux over the core. One can see the high level of flux in the beryllium reflector as well as flux drops in the irradiation sites.

IV.C. DONJON procedures

DONJON code is composed of a collection of modules, which call is controlled by CLE-2000 language. This environment allows an interpreted input where programming facilities are included as variables, loops, control statements and procedures. Modules interact with each other by objects. An object is a data structure, particular to a type ; for example, a geometry object is composed of a geometry type (Cartesian, cylindrical ...), meshes, material mixture number of each region etc.

In that context, inputs are constructed as programs and instructions are grouped in procedures. To realize a static calculation, a straightforward sequence of modules has to be called:

- **GEOD**: hexagonal geometry definition
- **CRE**: recovery of nuclear properties
- **TRIVAT**: tracking of the geometry
- **TRIVAA**: diffusion matrix assembly
- **FLUD**: diffusion equation solver

For input clarity, some variables can be defined as for number of regions or flux iteration precision. Even in a very simple case, these module calls can be divided in procedures: one for defining and tracking the geometry **PGEO**, one for recovering nuclear properties **PMAC**, and one to compute fluxes **FLUX**. The two first procedures are called object creation procedures ; when a geometry is defined, for any following static or even kinetics calculations, there is no use to re-execute the geometry definition procedure. The same logic is applied to property recovering.

When control devices are defined in the calculation, data structures for it must be constructed and can also be stored for further use. So a control rod is defined by **INIDE-V**; **INPROC**: modules and these modules compose **PROD** procedure. In Fig. 5, these procedure calls are shown. Circles represent objects ; doubled-line squares are procedures and single-line ones are modules. The creation procedures can be followed by a flux calculation as shown in the left side of the figure. If not, the resulting objects are stored and are directly accessed in later runs.

The left side of Fig. 5 illustrates the iterative possibility of a single input in DONJON. The procedure **MODROD** is used to set a new position for the rod with the module **LINKDS**:. The module **NEWMAC**: allows the calculation of actual mesh properties with respect to rod position.

V. NUMERICAL RESULTS

With the DONJON capabilities listed above, different calculations were carried out to study the HEU Slowpoke-2 reactor. Calculations for the control rod worth, the temperature reactivity coefficient of the reactor and the critical rod position depending on temperature were considered.

With the preceding reactor and control rod model, reactivity worth of the rod was computed. For a nominal core configuration (at 20°C), a reactivity worth of ≈ 5.3 mk was obtained whereas the experimental one is 5.4 mk. This result is almost independent of the microscopic library used in the DRAGON calculations as shown in Table 3.

One of the most important properties when determining the operating characteristics of a research reactor is its temperature reactivity coefficient. Experiments were done in the HEU Slowpoke-2 reactor at École Polytechnique to study the reactor behavior for various uniform temperatures.

In a first test to reproduce these measures, calculations were done in keeping the control rod outside of the reactor. Nuclear properties were thus computed with DRAGON at different temperatures from 10°C to 50°C . For each set of properties, static diffusion calculations were performed and excess reactivity is plotted in Fig. 6. For any available microscopic library used in DRAGON, the reactivity variation vs. uniform temperature curve is very much like the experimental one, while only calculations with ENDF/B5 library show a slope close to the measurements.

Nevertheless, reactivity levels are very different between microscopic libraries. Microscopic properties are not tabulated with the same temperatures in the three libraries, mainly for Beryllium isotope that compose the reactor reflector. Some libraries have also different isotopes for the same material, equivalence between these materials is difficult to assure.

To measure the temperature effect, the control rod position was noted and then reactivity was obtained from its reactivity calibration. Due to reactor configuration, the control rod absorbs neutrons only when it is located in the 8 lastest inches of its course. When the measures were made, the control rod was almost fully inserted and its maximal displacement was of one inch.

So the second test to reproduce measured data was the search for critical rod positions at each uniform temperature. The nuclear properties produced with DRAGON for the preceding test were used. Critical state of the reactor was chosen at 20°C for the rod inserted at 86.72% of full insertion, so ≈ 6 inches in the core.

For this reactor state, static calculations were done for properties from WIMS-AECL and ENDF/B5 libraries. The resulting multiplication factors represent critical values in the following search. Brent's method is then used to find the control rod position for which the reactor is critical, so K_{eff} is equal to the reference one. When using this method, two initial states must be found to bracket the root value.

To carry out this simulation in DONJON, rod reactivity worth vs position was drawn in order to find two rod positions for which K_{eff} is above and under the reference value. Fig. 7 shows the rod reactivity calibration. Calculations were performed at a uniform temperature of 20°C . The computation values are lower than the experimental data but reproduce a close curve.

Fig. 8 shows the rod position vs temperature as measured and as calculated. The three curves have the same shape. The values obtained with ENDF/B5 library are closer to the measured ones than the WIMS-AECL ones. In Fig. 6, the same observation is valid. Results with ENDF/B5 library give a smooth slope with respect to temperature while WIMS-AECL library ones show a greater reactivity difference between 10°C and 40°C values. As the control rod model represents the same reactivity worth as measured (Fig. 7), its movements to compensate for temperature reactivity increase are coherent.

VI. Conclusion

DONJON modular aspects allows complex static and time-dependent calculations in a single run and has proved to be useful to study core behaviors. CPU time needed to compute deterministic calculations is less than for probabilistic approach, and the results are reasonably accurate.

Even if geometric model of the reactor is less precise than in probabilistic codes, calculations with DRAGON/DONJON codes give good agreements with measurements. As DONJON code possesses kinetics capabilities, the next step in the HEU Slowpoke reactor study is to follow a day of operation or to look at power transients.

Acknowledgments — The authors would like to thank Dr. Greg Kennedy for providing experimental data. Part of this work was supported by a grant from the Natural Science and Engineering Research Council of Canada.

REFERENCES

- [1] A. Hébert (1987), "TRIVAC, A Modular Diffusion Code for Fuel Management and Design Applications," *Nucl. J. of Canada*, Vol. 1, No. 4, 325.
- [2] E. Varin, A. Hébert, R. Roy and J. Koclas (1996), "A User's Guide for DONJON," Report IGE-208, École Polytechnique de Montréal.
- [3] E. Varin, J. Koclas and R. Roy (1995), "Application of the DONJON Reactor Code for Regulating System Simulations", 19th CNS Simulation Symposium, Hamilton, Ontario.
- [4] G. Marleau, R. Roy and A. Hébert (1993), "DRAGON - A Collision Probability Transport Code for Cell and Supercell Calculations," Report IGE-157, École Polytechnique de Montréal.
- [5] A. Benaboud (1992), "Résolution de l'équation de la diffusion neutronique pour une géométrie hexagonale," Ph. D. Thesis, École Polytechnique de Montréal, Institut de Génie Énergétique .
- [6] A. Hébert (1986), "Preconditioning the Power Method for Reactor Calculations," *Nucl. Sci. and Eng.*, Vol. 94, 1.
- [7] C. Guertin (1991), "Calcul du coefficient de température du réacteur Slowpoke-2," Master Thesis, École Polytechnique de Montréal, Institut de Génie Énergétique .
- [8] J.V. Donnelly (1986), "WIMS-CRNL, A User's Manual for the Chalk River Version of WIMS", AECL-8955, Atomic Energy of Canada Limited.

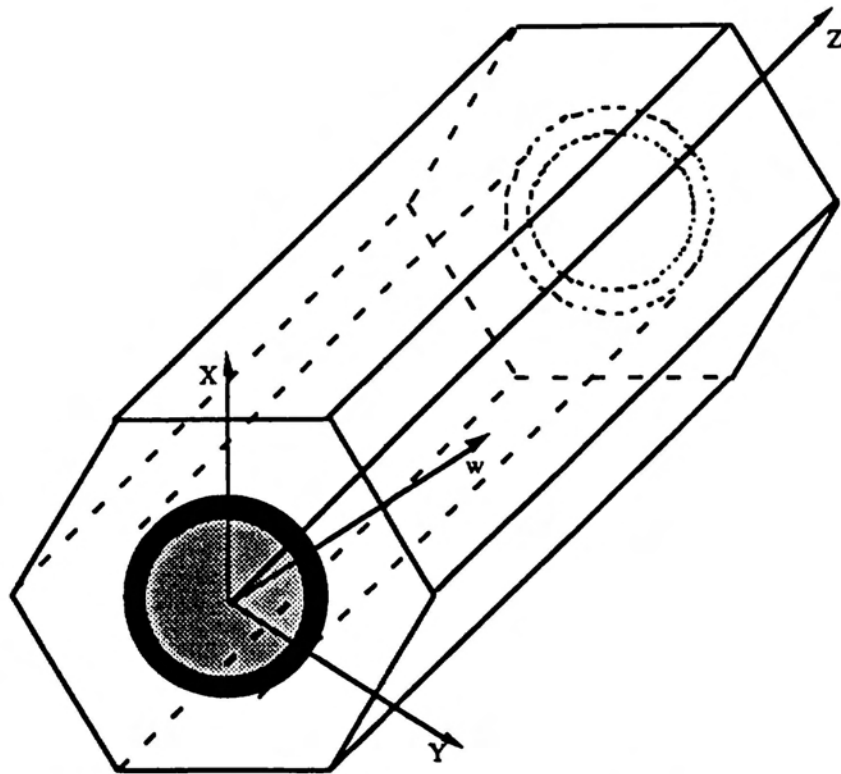


Figure 1: Main direction for a 3D hexagon

$$\begin{bmatrix}
 A_{11} & & & & \\
 -A_{21} & A_{22} & & & \\
 & -A_{32} & A_{33} & & \\
 & -A_{42} & -A_{43} & A_{44} & -A_{45} \\
 & & & -A_{54} & A_{55}
 \end{bmatrix}
 \begin{bmatrix}
 \vec{\Phi}_1 \\
 \vec{\Phi}_2 \\
 \vec{\Phi}_3 \\
 \vec{\Phi}_4 \\
 \vec{\Phi}_5
 \end{bmatrix}
 - \frac{1}{K_{\text{eff}}}
 \begin{bmatrix}
 B_{11} & B_{12} & B_{13} & B_{14} & B_{15} \\
 B_{21} & B_{22} & B_{23} & B_{24} & B_{25} \\
 & & & & \\
 & & & & \\
 & & & &
 \end{bmatrix}
 \begin{bmatrix}
 \vec{\Phi}_1 \\
 \vec{\Phi}_2 \\
 \vec{\Phi}_3 \\
 \vec{\Phi}_4 \\
 \vec{\Phi}_5
 \end{bmatrix}
 =
 \begin{bmatrix}
 \vec{0} \\
 \vec{0} \\
 \vec{0} \\
 \vec{0} \\
 \vec{0}
 \end{bmatrix}$$

Figure 2: Example of a 5-group matrix eigenvalue problem

Table 1: CPU Time in comparison with energy groups.
 Computation realized on one scalar node of the SP2 at EPM.

# energy groups	CANDU reactor	Slowpoke reactor
	6000 unknowns/energy group	50000 unknowns/energy group
	time (s)	time (s)
2	7	102
4	17	255
6	-	397
8	-	663

Table 2: Upper limit of each energy group

	Upper limit (eV)			
	with 2 groups	with 4 groups	with 6 groups	with 8 groups
Fast groups	1.00E+07	1.00E+07	1.00E+07	1.00E+07
	-	5.53E+03	8.21E+05	8.21E+05
	-	-	5.53E+03	5.53E+03
	-	-	-	2.77E+01
Thermal groups	4.00E+00	4.00E+00	4.00E+00	4.00E+00
	-	6.25E-01	6.25E-01	6.25E-01
	-	-	1.00E-01	2.20E-01
	-	-	-	5.00E-01

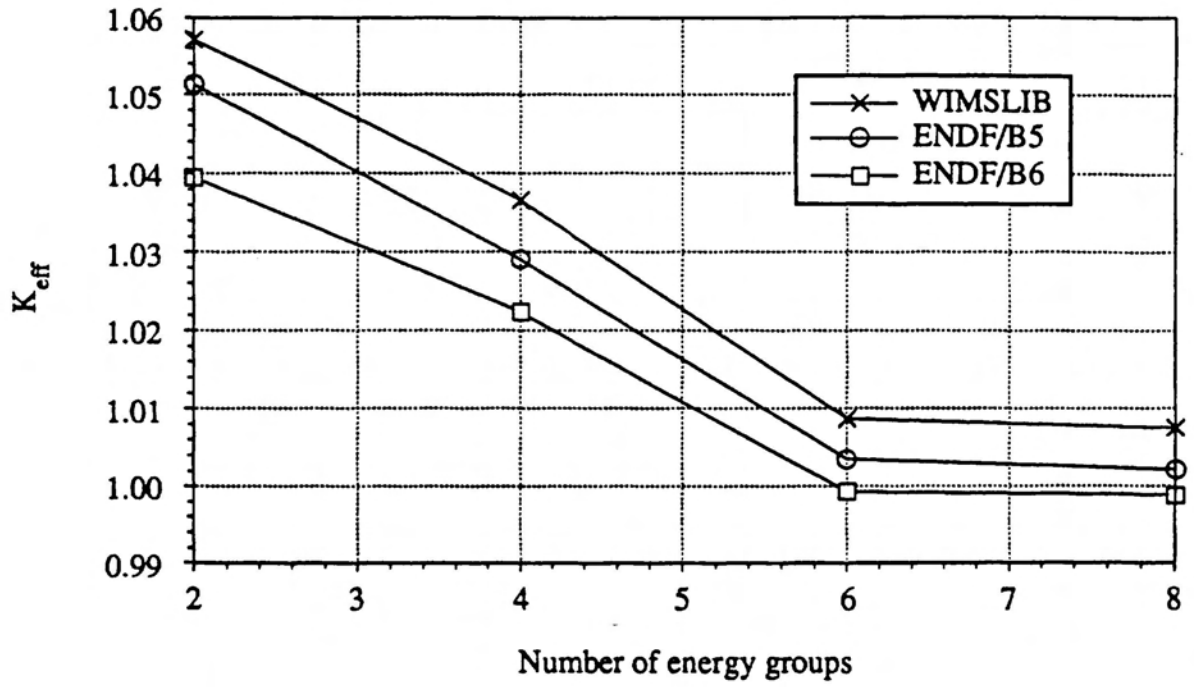


Figure 3: Energy group convergence

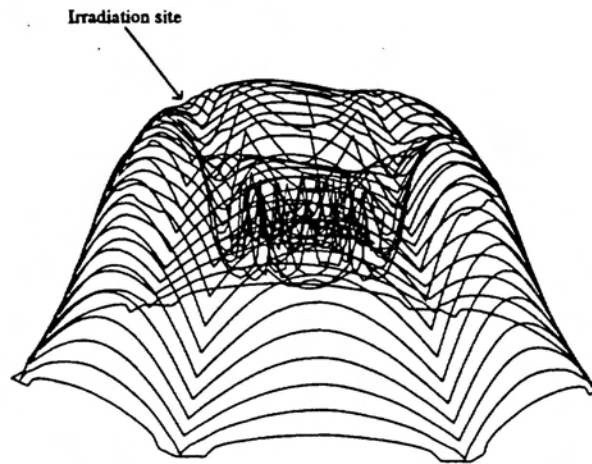


Figure 4: Most thermal flux in the Slowpoke-2 reactor.

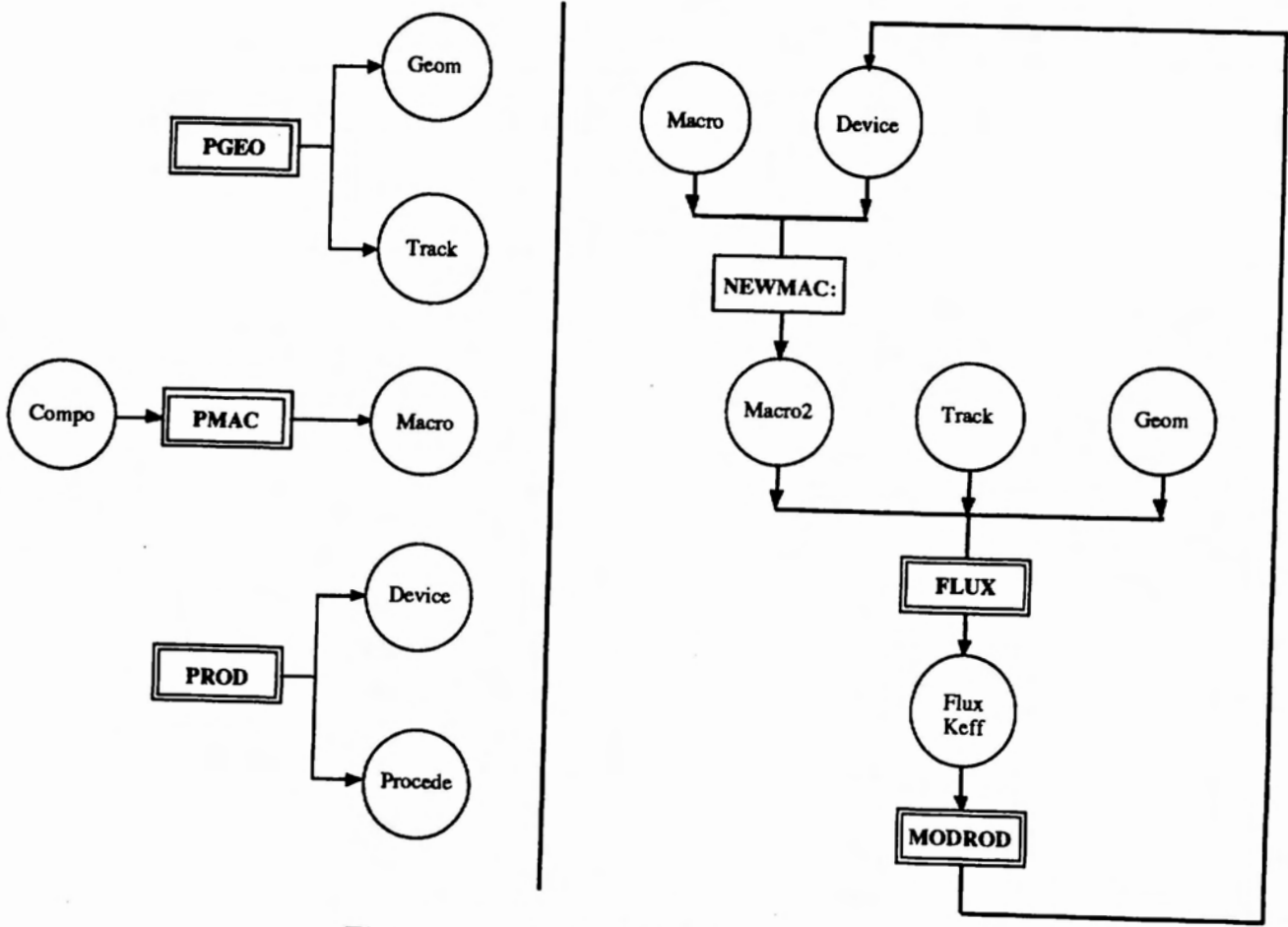


Figure 5: DONJON procedure calls.

Table 3: Control rod worth 6 energy groups, 20°C

Microscopic Library	Control rod worth (mk)
WIMSLIB	5.3
ENDF-B5	5.4
ENDF-B6	5.5

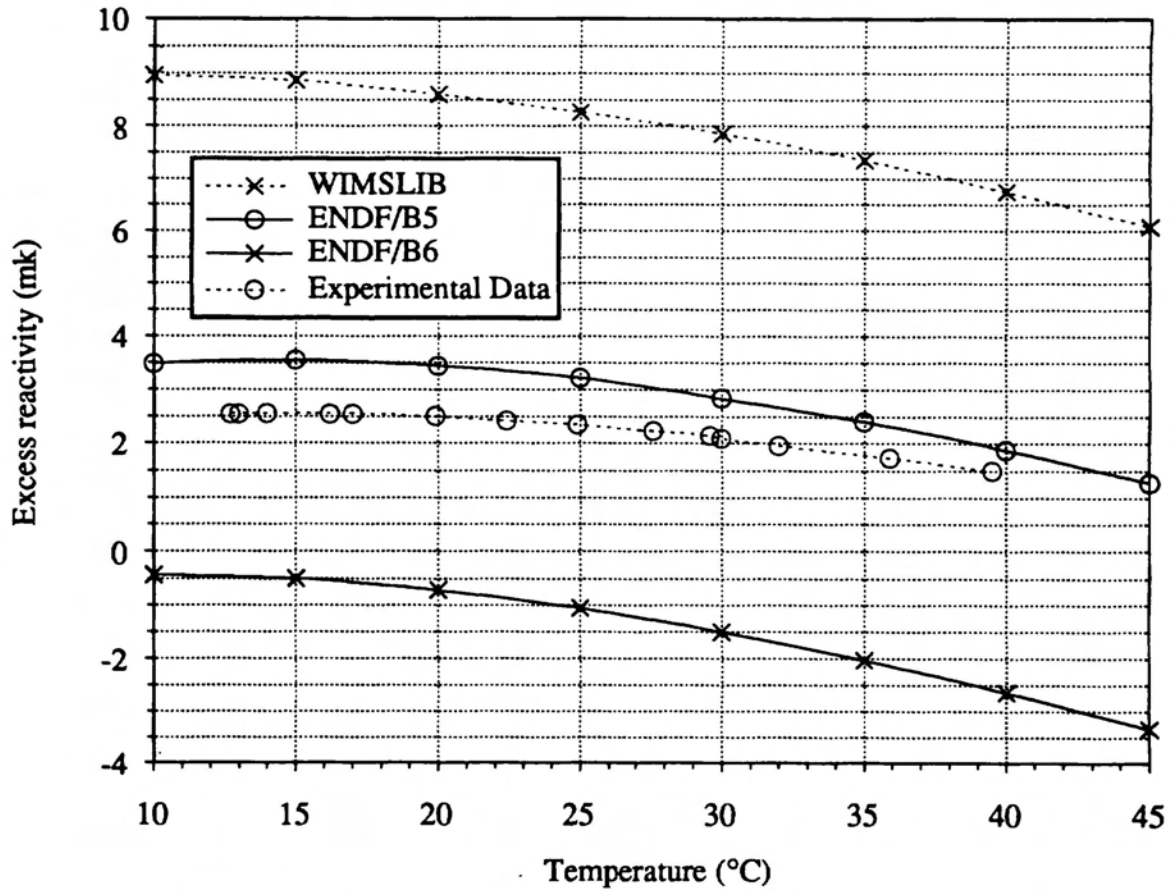


Figure 6: Temperature Reactivity for HEU Slowpoke reactor

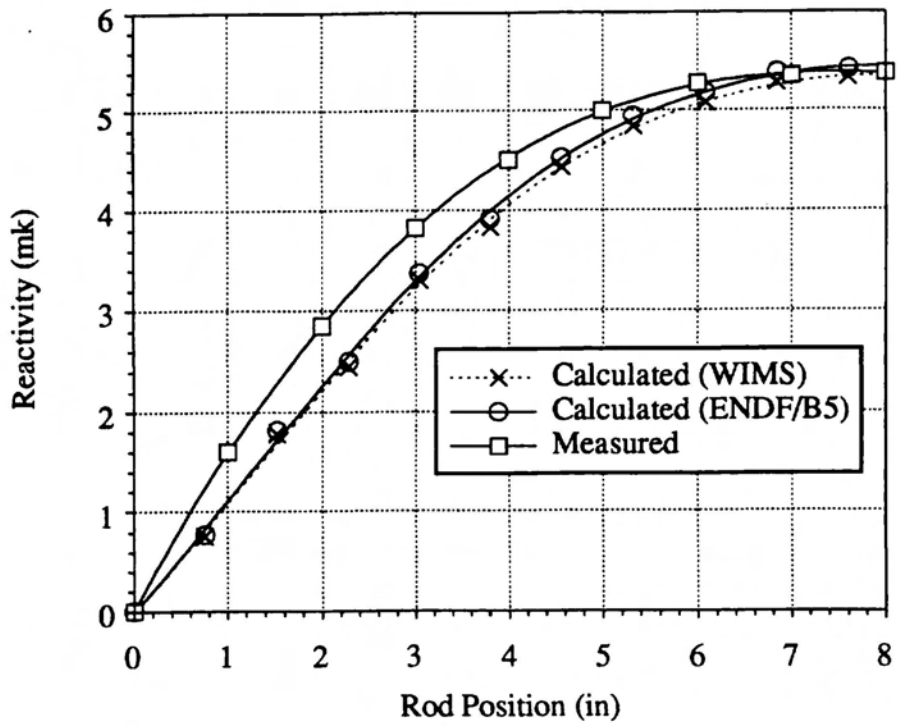


Figure 7: Control rod reactivity calibration

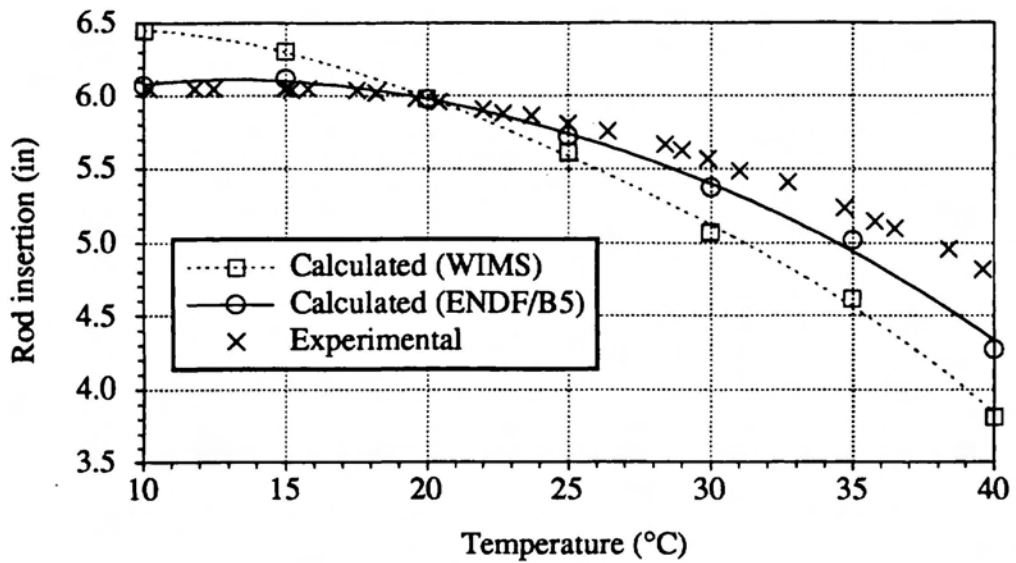


Figure 8: Control rod critical position